Biochimica et Biophysica Acta 1860 (2017) 685–694

Contents lists available at ScienceDirect

Biochimica et Biophysica Acta

journal homepage: www.elsevier.com/locate/bbagrm

Expression of *Rac1* alternative 3′ UTRs is a cell specific mechanism with a function in dendrite outgrowth in cortical neurons

Sandra Oliveira Braz [a,1], Andrea Cruz [a,b,1], Andrea Lobo [c,d,1], Joana Bravo [c,d,e], Joana Moreira-Ribeiro [c,d], Isabel Pereira-Castro [a,d], Jaime Freitas [a,d], Joao B. Relvas [b,d,*], Teresa Summavielle [c,d,**], Alexandra Moreira [a,d,f,***]

[a] *Gene Regulation Group, IBMC - Instituto de Biologia Celular e Molecular, Porto, Portugal*
[b] *Glial Cell Biology Group, IBMC - Instituto de Biologia Celular e Molecular, Porto, Portugal*
[c] *Addiction Biology Group, IBMC - Instituto de Biologia Celular e Molecular, Porto, Portugal*
[d] *Instituto de Investigação e Inovação em Saúde (i3S), Universidade do Porto, Porto, Portugal*
[e] *FMUP-Faculdade de Medicina da Universidade do Porto, Portugal*
[f] *ICBAS-Instituto de Ciências Biomédicas Abel Salazar, Universidade do Porto, Portugal*

ARTICLE INFO

Article history:
Received 19 September 2016
Received in revised form 2 March 2017
Accepted 3 March 2017
Available online 6 March 2017

Keywords:
Alternative polyadenylation
Cortical neuron differentiation
Neurite outgrowth
Rac1

ABSTRACT

The differential expression of mRNAs containing tandem alternative 3′ UTRs, achieved by mechanisms of alternative polyadenylation and post-transcriptional regulation, has been correlated with a variety of cellular states. In differentiated cells and brain tissues there is a general use of distal polyadenylation signals, originating mRNAs with longer 3′ UTRs, in contrast with proliferating cells and other tissues such as testis, where most mRNAs contain shorter 3′ UTRs. Although cell type and state are relevant in many biological processes, how these mechanisms occur in specific brain cell types is still poorly understood. Rac1 is a member of the Rho family of small GTPases with essential roles in multiple cellular processes, including cell differentiation and axonal growth. Here we used different brain cell types and tissues, including oligodendrocytes, microglia, astrocytes, cortical and hippocampal neurons, and optical nerve, to show that classical *Rho GTPases* express mRNAs with alternative 3′ UTRs differently, by gene- and cell- specific mechanisms. In particular, we show that *Rac1* originate mRNA isoforms with longer 3′ UTRs specifically during neurite growth of cortical, but not hippocampal neurons. Furthermore, we demonstrate that the longest *Rac1* 3′ UTR is necessary for driving the mRNA to the neurites, and also for neurite outgrowth in cortical neurons. Our results indicate that the expression of *Rac1* longer 3′ UTR is a gene and cell-type specific mechanism in the brain, with a new physiological function in cortical neuron differentiation.

1. Introduction

Alternative polyadenylation (APA) is a mechanism of gene regulation occurring in more than half of all mammalian genes that generates alternative 3′ UTR mRNA isoforms [1–3]. This regulatory mechanism comprises the formation of alternative 3′ ends of an mRNA by cleavage of the pre-mRNA and polyadenylation at different sites according to the polyadenylation signals (PASs). In the 3′ UTR, the usage of proximal or distal PAS has been correlated to global physiologic events and some diseases (reviewed in [4–8]). High-throughput sequencing technologies have allowed to identify APA-derived mRNA isoforms in different tissues, and a number of methods have been developed to more specifically analyze the 3′ ends of the transcripts ([1,9–12], reviewed in [13]). It has been shown that in proliferative cells there is a global preferential usage of proximal PASs [14,15], while during development and in differentiated cellular states there is preferential utilization of distal PASs [16,17]. It has been also shown that ubiquitously transcribed genes depend on APA for tissue-specific expression [12]. The 3′ UTR acts as a platform for RNA binding proteins (RBPs) and miRNA targeting, not only regulating the fate of the correspondent mRNA (reviewed in [18]) and protein production [19], but also the localization of the translated protein [20,21]. It was initially shown that distal PASs were preferentially used in the brain originating longer 3′ UTRs [22] and these observations were later studied [17,22–24]. However, brain tissues contain many different types of cells with distinct functions and the role of alternative 3′ UTRs in different primary brain cells is still poorly understood.

* Correspondence to: J. B. Relvas, Glial Cell Biology Group, IBMC - Instituto de Biologia Celular e Molecular, Instituto de Investigação e Inovação em Saúde (i3S), Universidade do Porto, Porto, Portugal.
** Correspondence to: T. Summavielle, Addiction Biology Group, IBMC - Instituto de Biologia Celular e Molecular, Instituto de Investigação e Inovação em Saúde (i3S), Universidade do Porto, Porto, Portugal
*** Correspondence to: A. Moreira, Gene Regulation Group, IBMC - Instituto de Biologia Celular e Molecular, Instituto de Investigação e Inovação em Saúde (i3S), Universidade do Porto, Porto, Portugal.
E-mail addresses: jrelvas@ibmc.up.pt (J.B. Relvas), tsummavi@ibmc.up.pt (T. Summavielle), alexandra.moreira@ibmc.up.pt (A. Moreira).
[1] These authors contribute equally to the work.

http://dx.doi.org/10.1016/j.bbagrm.2017.03.002
1874-9399/

Genes that produce mRNAs with multiple 3′ UTR and are ubiquitously expressed in different tissues have a function in regulatory processes, such as signaling, and regulate their protein expression by modulating their 3′ UTRs [12]. As differentiated brain cells are polarized cells containing specialized subcellular sections, the longer 3′ UTRs typically expressed in brain tissues are certainly associated with mechanisms of post-transcriptional regulation, such as mRNA transport and localization (reviewed in [25]). This has been clearly demonstrated in the hippocampus where the *Bdnf* (brain-derived neurotrophic factor) 3′ UTR plays a function in spine morphology and synaptic plasticity [26] and notably, learning and memory were shown to be regulated by the transport of specific mRNAs such as MAP2, calmodulin, Pumilio and eEF1A to axons and dendrites [27–30].

Rho (Ras homologue) family of small guanosine triphosphatases (Rho GTPases) includes a large subgroup of the Ras superfamily of 20–30 kDa GTP-binding proteins [31], comprising the family of the classical RhoA (Ras homolog gene family, member A)-, Rac1 (Ras-related C3 botulinum toxin substrate 1)- and Cdc42 (Cell division control protein 42 homolog)-related subfamilies [32,33]. Rho GTPases integrate signals from the environment to intracellular signal transduction pathways, thereby controlling a wide range of essential biochemical responses in eukaryotic cells [34]. They act as binary molecular switches by cycling between an inactive GDP-bound state and an active GTP-bound conformation [35]. When activated, these GTPases interact with their downstream effectors, which in turn regulate a wide range of mechanisms such as microtubules dynamics, transcription activation or membrane trafficking. These interactions, as well the resulting functions, are likely to be specific for each cell-type and physiologic condition. Rho GTPases are therefore fundamental for diverse cellular processes including cell growth, cytokinesis, cell motility, cell adhesion, cell transformation, invasion and neuronal development [34,36,37]. However, the co-transcriptional mechanisms that regulate the expression of these genes are mostly unknown.

Here, we mapped the alternative 3′ UTRs of several members of the Rho GTPase family, including *Rac1*, *Cdc42* and *RhoA*, in different types of brain primary cells, including oligodendrocytes, cortical and hippocampal neurons, microglia and astrocytes. We observed that the alternative 3′ UTR pattern changes in a gene- and cell- specific manner, and that for *Rac1* this has functional consequences. Our results clearly indicate that the expression of *Rac1* longest mRNA isoform increases during neurite growth in cortical neurons, concomitant with protein expression. We show that *Rac1* longer 3′ UTR mRNA is highly expressed in the dendrites of cortical neurons, but not in the hippocampal neurons. We also show that the longer 3′ UTR produced by distal PAS selection is essential for targeting *Rac1* mRNA to neurites and for neurite outgrowth in cortical neurons.

2. Results and discussion

2.1. Rho GTPases produce two alternative polyadenylation mRNA isoforms with different 3′ UTRs

We have previously shown that Rho GTPases are critical players in oligodendrocyte (OL) differentiation [38], however, the molecular mechanisms regulating their expression during that cellular process are still poorly understood. *Rac1*, *RhoA* and *Cdc42* genes contain putative PASs in their 3′ UTRs. To map and characterize the multiple 3′ UTR mRNA isoforms produced by *Rho GTPases* in specific brain cells, we used 3′ RACE/sequencing to identify the mRNA 3′ ends of *Rac1*, *RhoA* and *Cdc42* in rat primary oligodendrocytes differentiated *in vitro* for three days, and also in OLN93 and CG4 oligodendrocyte cell lines (Fig. 1A–C and Supplementary Figs. 1–2). *Cdc42* produces two alternatively spliced isoforms, *Cdc42Iso1* and *Cdc42Iso2* and their mRNA 3′ ends were individually mapped using specific primers (Supplementary Fig. 1A). In differentiated oligodendrocytes, *Rac1*, *RhoA* and *Cdc42Iso1* are transcribed in two main mRNA isoforms due to the use of the two putative PASs localized in their 3′ UTR, while *Cdc42Iso2* produces only one mRNA isoform (Fig. 1B). OLN93 and CG4 cell lines present similar *Rac1* and *RhoA* APA-derived mRNA isoforms to those presented by OLs, but distinct *Cdc42Iso1* and *Cdc42Iso2* mRNA isoforms (Supplementary Fig. 1B), which indicates that for *Cdc42* APA is a cell specific mechanism. The 3′ mapping shows that the shorter *Rac1* mRNA isoform is produced by cleavage and polyadenylation of the pre-mRNA at the dinucleotide CA (red bar, Fig. 1C), which is the optimal consensus cleavage site that is preceded by the AUUAAA (here named *Rac1* pA1), a close variant of the canonical PAS [39,40]. The longer mRNA isoform is produced by usage of by the distal canonical PAS, AAUAAA (here named *Rac1* pA2) (Fig. 1C).

Genome conservation analysis for the selected *Rho GTPases* revealed a surprisingly high conservation of the 3′ UTR between seven mammalian species: an identity above 72% for *Rac1* (Fig. 1D), and over 78% for *Cdc42 Iso1*, *Cdc42 Iso2* and *RhoA* (Supplementary Fig. 2). Interestingly, all PASs show approximately 100% pairwise identity, with the exceptions of *Rac1* pA1 and *RhoA* pA2, which present a single mismatch in the marsupial Tasmanian devil and thus have a 95.8% conservation. All species analysed show a 100% conservation in *Cdc42iso1* pA1, with the exception of Tasmanian devil (Fig. 1D and Supplementary Fig. 2B). This high level of conservation suggests that the 3′ UTRs and the PASs have relevant functions in Rho GTPases polyadenylation and expression in mammalians, and this holds true even in marsupials, which were separated from placental mammals more than 160 million years ago [41].

2.2. Rho GTPases alternative 3′ UTRs expression during oligodendrocyte differentiation and optical nerve development

Genome-wide studies have shown that mammalian brain tissues present higher expression of APA-derived mRNAs with longest 3′ UTRs [17,22,23]. However, brain tissues contain different cell populations and it has also been recently shown that single mouse embryonic and neural stem cells differ in the choice of APA-derived isoforms [42]. Therefore, we analysed *Rac1*, *Cdc42Iso1*, *Cdc42Iso2* and *RhoA* mRNAs by RT-qPCR in different brain primary cell types and tissues, specifically, in oligodendrocytes precursor cells (OPC) (0d), OLs differentiated *in vitro* for 3, 5 and 7 days, optical nerve at different developmental stages, microglia, astrocytes, cortical and hippocampal neurons. Two specific primer pairs were designed to quantify total mRNA expression (referred as CDS) and the expression of the longest mRNAs isoform (referred as pA2) for each gene (Fig. 2A). We observed that for all the genes analysed the pA2/CDS (total) expression ratios are not significantly altered, suggesting that the longest 3′ UTRs are not preferentially expressed, during all the accessed differentiation states of the oligodendrocytes (Fig. 2B).

Rho GTPases act by integrating signals from the environment, consequently their expression and regulation may be modulated by extracellular cues. Although the *in vitro* culture conditions try to reproduce as most as possible the *in vivo* context, we do not exclude the possibility that distal PASs selection may be activated by extracellular signals. Thereby, we collected rat optic nerve (ON), which are mainly composed by OLs [43], at postnatal (P) time points (P2, P14 and P30) to confirm the results obtained at d0, d3 and d5-7 with the OPC/OL differentiating cultures. We observed that the trend in *Rac1, Cdc42Iso1, Cdc42Iso2* and *RhoA* pA2/CDS expression ratios in ONs (Fig. 2C) is consistent with that observed in OL cell cultures (Fig. 2B).

It has been previously shown that there is a preferential usage of distal PASs in brain tissues [17,23], however we do not observe this effect for *Rho GTPases* in primary oligodendrocytes during *in vitro* or *in vivo* differentiation. This suggests that 'classically' activated *Rho GTPases* do not use an APA switch towards the distal PASs as a regulatory mechanism of gene expression during OL differentiation. It is possible that the preferential expression of 'classical' *Rho GTPases* mRNAs containing shorter 3′ UTRs is related to a particular function for the correspondent proteins in OL differentiation, and one possible explanation for our findings may reside in the nature of this family of proteins. As they are

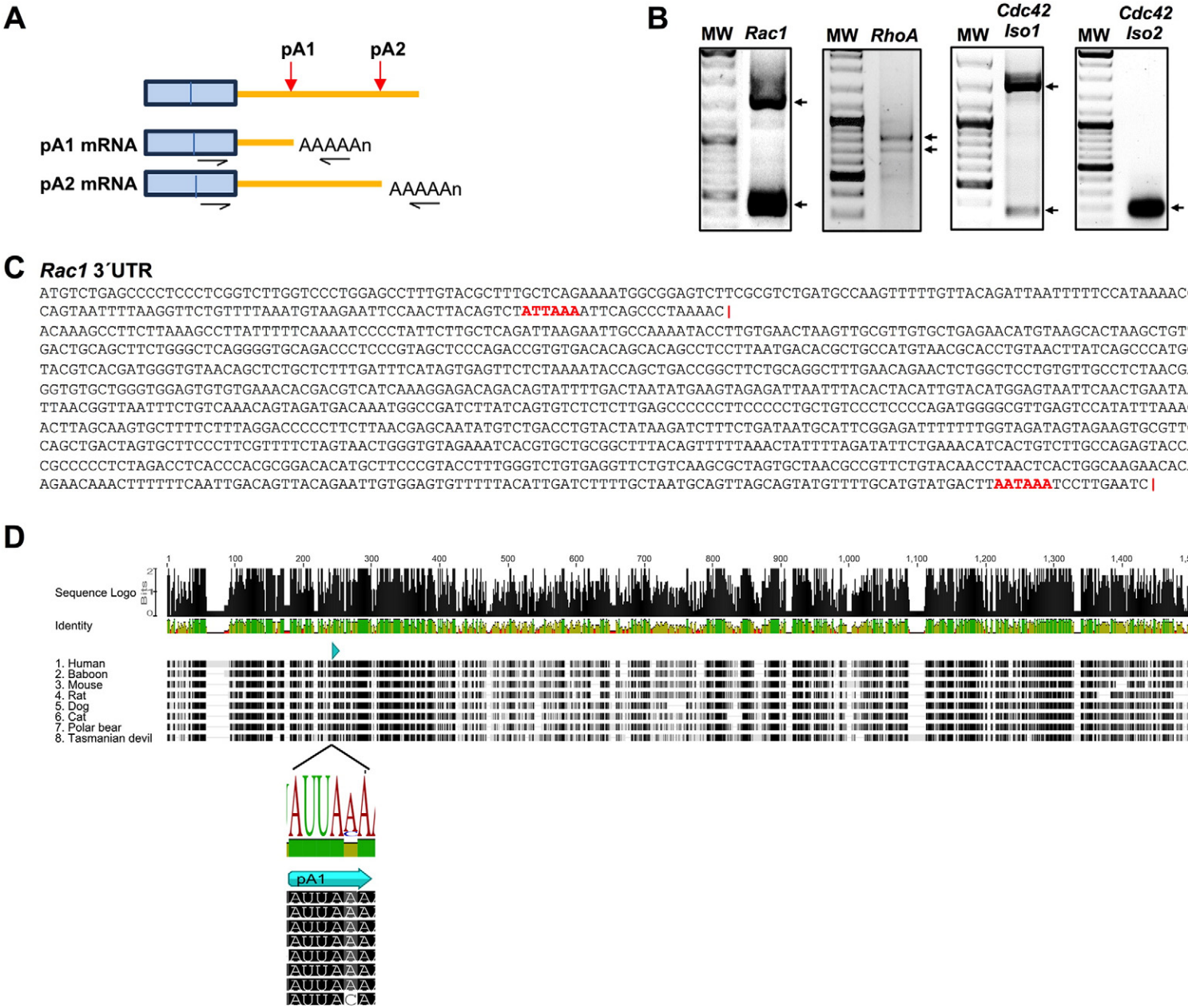

Fig. 1. Rho GTPases Rac1, Cdc42 and RhoA produce multiple 3′ UTRs mRNAs due to alternative polyadenylation. A. Schematic representation of two mRNAs derived from the usage of different PASs in the 3′ UTR (pA1 and pA2), and primers used in 3′ RACE. B. 3′ RACE representative gel. The first lane of each panel corresponds to the molecular weight DNA ladder (GeneRuler DNA Ladder Mix (Thermo Fisher) and the second lane shows the mRNA isoforms (arrows) of *Rac1*, *RhoA*, *Cdc42Iso1* and *Cdc42Iso2*, produced in primary oligodendrocytes. C. Sequencing results indicating PASs (bold and colored in red) and the correspondent PASs (red bar). D. Genomic alignment of *Rac1* 3′ UTR sequence in seven representative mammalian species. *Rac1* 3′ UTR presents above 72% conservation throughout the whole sequence and a close-up on the PASs (95.8% conservation) is shown.

regulated at the protein level by cycling between an inactive GDP-bound state and an active GTP-bound conformation, they may need to be highly expressed and do not require an additional level of regulation by producing a longer 3′ UTR.

To investigate *Rho GTPases* alternative 3′ UTR expression in other type of glial cells, we analysed primary microglia (Fig. 2D), and astrocyte cultures (Fig. 2E). We observed that *Rac1*, *Cdc42Iso1*, *Cdc42Iso2 and RhoA* present higher relative expression of CDS than pA2 mRNAs in both microglia and astrocytes. It has been shown by genome wide studies that in *Drosophila* CNS there is a complete "switch" towards the distal PASs usage [17] in comparison to mammalian brains, where this switch is not complete [23] *i.e.*, although levels of longer mRNAs are higher, the shortest isoforms still continue to be expressed. It was hypothesized that these differences were due to the presence of a higher percentage of glial cells in mammalian brain than in the *Drosophila* CNS [23] and our results for *Rho GTPases* in OLs, microglia and astrocytes support this hypothesis.

2.3. Rac1 longest 3′ UTR mRNA isoform is highly expressed during neurite growth of cortical neurons

To further explore the cellular specificity of *Rho GTPases* APA we assessed PASs usage in rat cortical (Fig. 3A) and hippocampal (Fig. 3B) neurons by RT-qPCR using the same strategy as above. For *Cdc42 Iso1*, *Cdc42 Iso2*, and *RhoA*, the expression pattern in both types of neurons shows no significant changes in the isoforms ratio during neurite growth. However, for *Rac1* mRNA, we observed a distinct pattern between cortical and hippocampal neurons (Fig. 3). In cortical neurons there is a significant increase in the pA2/CDS ratio of expression during neurite growth (Fig. 3A), that is not observed in hippocampal neurons

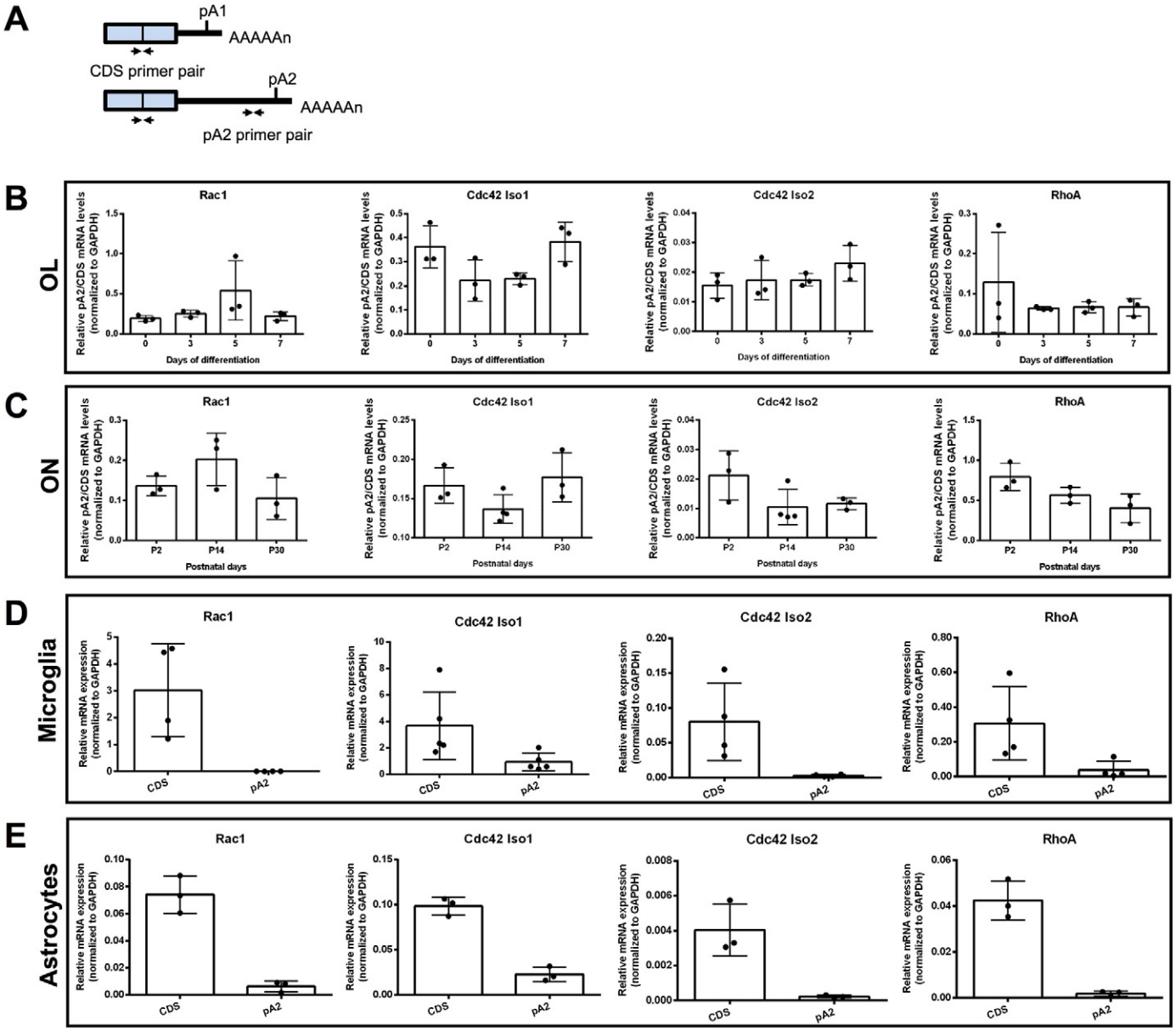

Fig. 2. Rho GTPases mRNAs expression in primary glial cells. A. Schematic mRNA sequence of *Rac1*, *Cdc42Iso1*, *Cdc42Iso2* and *RhoA*, depicting the primer pairs used in RT-qPCR to amplify both mRNA isoforms (CDS) and the longer mRNA isoform (pA2 primer pair). B–C. Ratios of the relative pA2/CDS mRNA expression levels of *Rac1*, *Cdc42Iso1*, *Cdc42Iso2* and *RhoA* quantified by RT-qPCR in B. primary OPC/OL at 0, 3, 5 and 7 days of differentiation, C. ON at P2, P14 and P30 days postnatal, D–E. Relative mRNA expression levels of *Rac1*, *Cdc42Iso1*, *Cdc42Iso2* and *RhoA* quantified by RT-qPCR D. Primary microglia cultures and E. Primary astrocytes cultures. mRNA levels were normalized for GAPDH mRNA. Data show the mean ± standard deviation (SD) for at least three independent experiments.

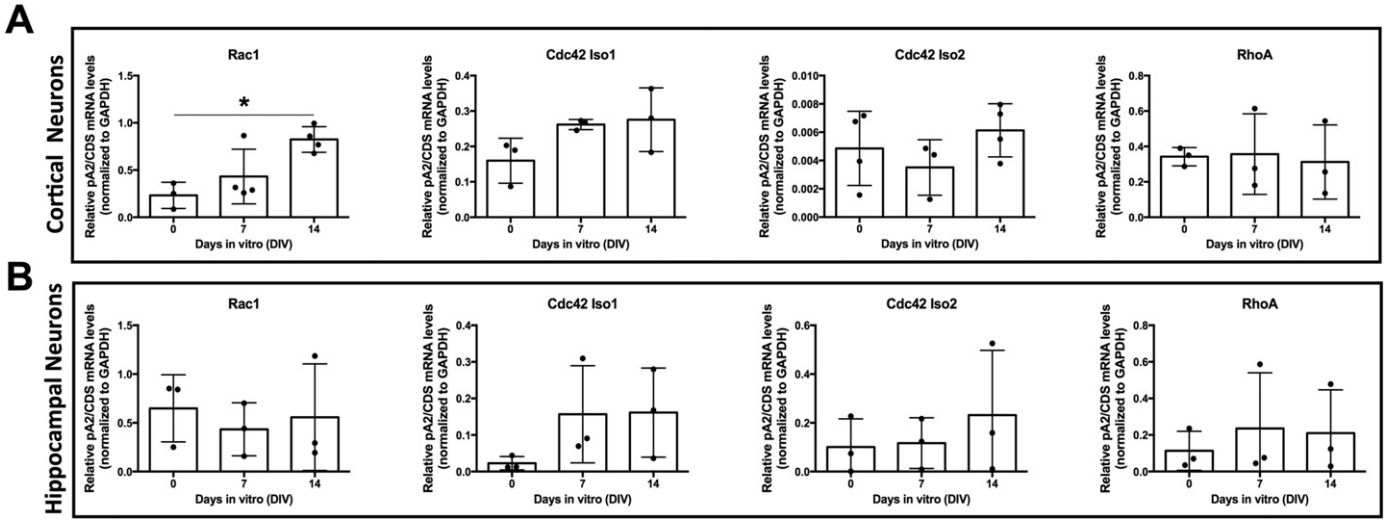

Fig. 3. *Rac1* longest 3′ UTR mRNA expression increases during neurite outgrowth in primary cortical neurons. Ratios of the relative pA2/CDS mRNA expression levels for *Rac1*, *Cdc42Iso1*, *Cdc42Iso2* and *RhoA* quantified by RT-qPCR in A. primary cortical and B. hippocampal neurons. The mRNA levels were normalized for GAPDH mRNA. Data show the mean ± standard deviation (SD) for at least three independent experiments. Data was analyzed by one-way analysis of variance (ANOVA) followed by Sidak *multiple comparison post-hoc* test ($^{*}p < 0.05$).

(Fig. 3B). Of note, this increase in the expression of the Rac1 longest mRNA isoform is statistically significant between d0 and d14 in cortical neurons. The reason why we observe this difference between cortical *vs* hippocampal neurons is still unclear but possibly reflects cell intrinsic properties or environment signaling. Although the described roles for Rac1 protein in both cell types are related to the process/dendrite extension, Rac1 is also important for axonal maintenance. Axons are particularly long structures and Rac1 may need a differential regulation for the proper outgrowth and maintenance of this structure. Our data also indicate that genes coding for the same family of proteins can undergo different co- or post-transcriptional regulatory mechanisms in different cell types. Overall, our results indicate that APA is a cell-type and gene-specific mechanism that fine-tunes gene expression. Furthermore, these data suggest a connection between the usage of alternative 3′ UTRs and the function of ubiquitously expressed genes in each type of cell.

2.4. Rac1 longest 3′ UTR mRNA isoform is localized in dendrites of primary cortical neurons and is associated with protein localization

APA-derived alternative 3′ UTRs regulate localization, stability and translation of their mRNAs [19–21]. This is the case of the well-known BDNF, where the longer mRNA isoform localizes at the dendrites and affects their normal development and function [26]. Transcriptome analysis of neural projections and soma have recently revealed that the majority of the mRNAs localized in cortical neurites express the longest 3′ UTRs [24]. To investigate the function of the different *Rac1* APA-derived 3′ UTRs in primary cortical and hippocampal neurons, we used a Boyden chamber to separate the soma from the neurites of the neurons (Fig. 4A). mRNA was extracted from the soma and dendrites from cortical and hippocampal neurons, and the expression of *Rac1* mRNA isoforms analyzed by RT-qPCR. Interestingly, we observed an enrichment of the longest *Rac1* mRNA (pA2) in cortical neurons in comparison to total mRNA (CDS), which is not observed in hippocampal neurons (Fig. 4B). Our results are consistent with the RNA-Seq data obtained with N2A cells, a cell line that was shown to faithfully reproduce primary cortical neurons in gene expression [24], confirming *Rac1* mRNA enrichment in the neurites (accession GSE67828). Furthermore, our results indicate that *Rac1* longest mRNA localizes specifically in the neurites of primary cortical neurons, but not in hippocampal neurons, and thus that this mechanism is cell-specific. To better understand the function of the multi 3′ UTR *Rac1* mRNA isoforms, we transfected cortical neurons with GFP-tagged plasmids containing the different *Rac1* 3′ UTR (GFP-Rac1 pA1 3′ UTR, containing the shortest *Rac1* 3′ UTR, and GFP-Rac1 pA2 3′ UTR, containing the longest *Rac1* 3′ UTR, where pA1 was mutated in order to use the distal PASs and produce the longest 3′ UTR). Our results show that GFP-Rac1 pA2 3′ UTR localizes preferentially in the neurites while the GFP-Rac1 pA1 3′ UTR, containing the shorter 3′ UTR, localizes in the soma (Fig. 4C and Sup. Fig. 3).

Overall these results indicate that *Rac1* APA-derived 3′ UTR mRNA isoforms are differentially expressed in different types of neurons, that this mechanism is cell specific and has a function in fine-tuning gene expression of this *Rho GTPase*. Furthermore, these data show a correlation between alternative PASs usage and their function in a particular type of cell.

2.5. The longest Rac1 3′ UTR is necessary for neurite outgrowth

To investigate whether the *Rac1* longest 3′ UTR was directly involved in the regulation of cortical neurite outgrowth, we knocked down (KD) its expression in primary cortical neuronal cultures using a lentiviral shRNA vector. Control cultures were infected with lentivirus carrying a shRNA against the dsRED fluorescent protein. Both experimental (shRac1 long 3′ UTR) and control dsRED lentiviral vectors also encoded green fluorescent protein (GFP), which was expressed throughout the entire infected neuron bodies, including the neurites (Fig. 5A). Primary cortical neurons were infected at day 1 and the cultures were analysed 7 (DIV7) and/or 14 (DIV14) days after transduction. Western blot analysis of protein lysates obtained from those cultures revealed that knocking down Rac1 longest 3′ UTR led to a significant reduction of total Rac1 protein levels compared with those of dsRED infected controls at both DIV7 and 14 (Fig. 5B) indicating that this isoform contributes for protein production. Our results show that while knocking down the *Rac1* long 3′ UTR mRNA isoform in cortical neurons did not affect the number of primary neurites formed (Fig. 5C), it significantly reduced their length (Fig. 5C), and changed their morphological characteristics, reducing their arbour complexity, as quantified by Sholl analysis (Fig 5E), compared with controls (shRNA dsRED) at DIV7.

The reduction in the total levels of Rac1 (Fig. 5B) *per se* could influence neurite outgrowth. Therefore, to demonstrate the specificity of the effects on neurite length and arbour complexity mediated by knocking down the long 3′ UTR *Rac1* mRNA isoform, we performed rescue experiments. In these experiments we transfected cortical neurons that had been KD for the long 3′ UTR *Rac1* mRNA isoform, with a plasmid where the *Rac1* 3′ UTR had the proximal polyA signal mutated to ensure that only the longer mRNA isoform was produced. This plasmid

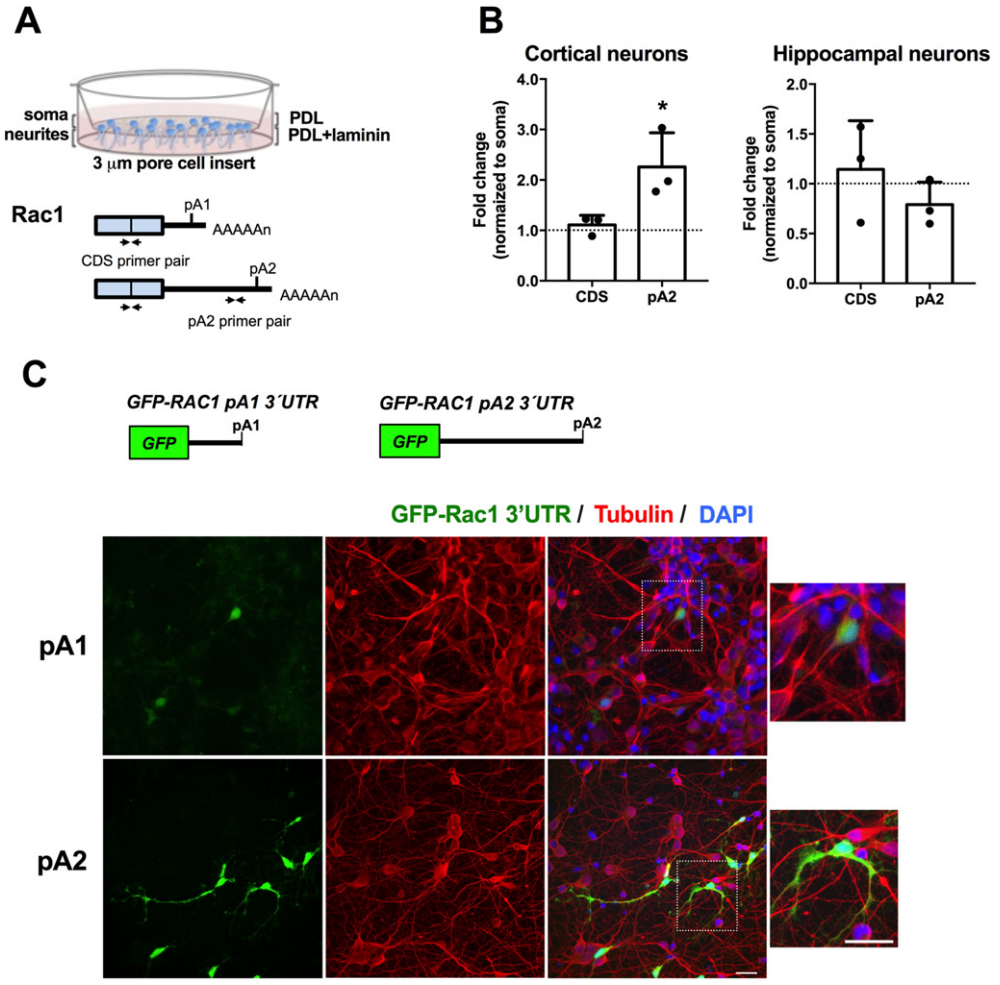

Fig. 4. *GFP-Rac1* longest 3′ UTR localizes in the neurites of primary cortical neurons. A. Schematic representation of the Boyden chamber; scheme of *Rac1* mRNA, depicting the primer pairs used in RT-qPCR to amplify both mRNA isoforms (CDS primer pair) and the longer mRNA isoform (pA2 primer pair). B. Quantification of both *Rac1* mRNAs (CDS) and the pA2 mRNA isoform (pA2) by RT-qPCR, using RNA extracted independently from the soma and neurites fractions of primary cortical and hippocampal neurons cultured in Boyden chambers. Data show the mean ± standard deviation (SD) for at least three independent experiments. Comparisons were performed against dsRed control values using a paired Student's *t*-test ($^{*}p < 0.05$). C. Immunofluorescence representative images of primary cortical neurons transfected at DIV 1 with pEGFP-tagged constructs containing *GFP-Rac1* pA1 3′ UTR and *GFP-Rac1* pA2 3′ UTR, showing that EGFP-Rac1 pA1 3′ UTR is predominately localized in the soma while EGFP-Rac1 pA2 3′ UTR is localized along the neurites. Tubulin was used to label microtubules and 4′-6-diamidino-2-phenylindole (DAPI) for the nucleus. Scale bars represent 50 μm.

also encoded mCherry, allowing visual identification of transfected cells (in red) and double transduced neurons (yellow) (Fig. 5D). Our results show that overexpressing the long 3′ UTR *Rac1* isoform significantly increased both the total neurite length (Fig. 5F), and their arbour complexity at DIV14 (Fig. 5E).

Rac1 protein expression has been shown to be responsible for dendrite outgrowth in cortical neurons [44]. Our findings now point towards an important physiological function for *Rac1* APA specific for cortical neurons: *Rac1* longer 3′ UTR mRNA contributes to Rac1 protein production, specifically correlates to increased levels of the protein in neurites, and is necessary for their outgrowth and for arbour complexity.

Overall, our work reveals that alternative 3′ UTR expression is a gene- and cell-specific mechanism, which should be considered when analyzing genome-wide data obtained with tissues composed by a mixture of cell types. Our results also demonstrate that in specific brain cell types, alternative 3′ UTRs allows a tight cell-specific regulation of genes that are ubiquitously expressed, with a function in cell physiology.

3. Materials and methods

In silico analysis. The UCSC genome browser was accessed to check for APA sites of human mRNAs. The nucleotide sequences were obtained from NCBI or Ensembl databases. Conservation of nucleotide sequences among different species was performed by multiple sequence alignment using the default settings of the MUSCLE 3.6 software implemented on Geneious v4.8 [45]. The mRNAs or gene accession numbers used in the sequence alignments are listed in Supplementary Table S1.

Cell Cultures: Primary mixed glial cultures (composed of OPC, microglia and astrocytes) were harvested from post-natal day (P) 1 to P2 neonatal Wistar rat cortex following a standard protocol [46] with minor modifications [47]. In brief, dissociated rat neonatal cortices were cultured *in vitro* for 10 days at 37 °C in 7.5% CO_2 in DMEM with 10% FCS and 1% penicillin/streptomycin. Microglia was removed from the top of the mixed glial cultures, for that the flasks were shaken for 1 h at 200 rpm on an orbital shaker. Microglia were plated at 1×10^6 cells per mL into 10 cm plate in DMEM/F12 supplemented with 1 ng/mL GM-CSF and 10% FBS media. The cells were left 24 h for recovery and adhesion, and were used directly for total RNA extraction. After the pre-shake, mixed glial cultures were shaken at 240 rpm overnight to dislodge the loosely attached OPC. These OPC were further purified from contaminating microglia by a differential adhesion step. Purified OPC were plated at a density of 20,000 cells per 0.8 cm^2/well in proliferation media in SATO media [L-glutamine (4 mM), putrescine (16 μg/mL), T4 (400 μg/mL), T3 (400 μg/mL), progesterone (6.2 ng/mL), sodium

selenite (5 ng/mL), BSA V (100 μg/mL), insulin (5 μg/mL), holo-transferrin (50 μg/mL)] supplemented with PDGF-AA (10 ng/mL), FGF-2 (10 ng/mL), 1% penicillin/streptomycin, 1% ITS and 0.5% FCS. After 2 days the cells are harvested, for day 0-time point, or maintained for induction of differentiation. The proliferation media was replaced with differentiation media (SATO media supplemented with 1% penicillin/streptomycin and 0.5% FCS). Cells were collected at 3, 5 or 7 days of differentiation. All cells were cultured in Poly-D-Lysin and Laminin (both from SIGMA-ALDRICH) coated plates. The astrocytes were recovered upon the third shake describe above, the mixed glial cultures were subject to trypsinization and plated in new flask for further astrocyte purification. A total of three steps of purification were performed. After obtaining a pure astrocytes culture, the cells were used directly for total RNA extraction.

Hippocampal and cortical neuronal cultures. E18 Wistar rat hippocampal and cortical neurons were cultured as previously described [48]. Briefly, after dissection, hippocampi or cortices were treated with trypsin (0.045%, 15 min, 37 °C, ThermoFisher Scientific) in Ca^{2+}- and Mg^{2+}-free Hank's balanced salt solution (HBSS; ThermoFisher Scientific), washed with HBSS containing 10% fetal bovine serum, to stop trypsin activity, and washed in HBSS to remove serum and avoid glia growth. Finally, the tissues were transferred to serum-free Neurobasal medium (ThermoFisher Scientific), supplemented with B27 (1:50, ThermoFisher Scientific), glutamine (0.5 mM, Sigma-Aldrich), gentamycin (0.12 mg/mL ThermoFisher Scientific), and glutamate (25 μM, Sigma-Aldrich) for the hippocampal neurons, and dissociated mechanically. Neurons were maintained in the supplemented Neurobasal medium on poly-D-lysine (PDL, 10 μg/cm^2; P0899, Sigma-Aldrich) coated 6 microwell plates at a density of 9×10^4 cells/cm^2 or on coverslips (10 mm) treated with nitric acid and coated with PDL (20 μg/cm^2) at a density of 8×10^4 cells/cm^2. For the separation of soma and neurite fractions, neurons were plated at a density of 9×10^4 cells/cm^2 on 3 μm pore polyethylene terephthalate (PET) membrane filter inserts (Corning) coated with PDL on both sides and with laminin (1 μg/cm^2, Sigma-Aldrich) on the bottom side of the insert to stimulate neurite crossing, as previously described [49]. Cells were kept at 37 °C in a humidified incubator with 5% CO_2/95% air, for 14 days, and half of the medium was replaced at day 7. All procedures necessary to obtain primary cell cultures were conducted in accordance with European regulations (European Union Directive 2010/63/EU) and were approved both by the Animal Ethics Committee of I3S-IBMC and the Portuguese regulatory entity — Direcção Geral de Alimentação e Veterinária (DGAV, ref 11769/2014-05-15 to TS). Animal facilities and the people directly involved in animal experiments (TS, JB, AL) were also certified by DGAV. All efforts were made to ensure minimal animal suffering.

RNA extraction and Real-time quantitative PCR (RT-qPCR). Cells were washed twice with ice-cold PBS and centrifuged for 5 min at 300 g at 4 °C. The cell pellet was resuspended in 1 mL TRIzol (Invitrogen) to extract total RNA. 500 ng RNA for each condition was treated with DNase I (Roche) following the manufacturer's instructions. cDNA was synthetized using Superscript III reverse transcriptase (Invitrogen) according to the manufacturer's protocol. RT-qPCR reactions were performed using SYBR Select Master Mix (Applied Biosystem) and following the manufacturer's instructions. The relative expression of RNA was calculated relative to the reference gene *GAPDH*. Primer sequences are presented in Supplementary Table S2.

3′ RACE analyses. The cDNA synthesis was performed using the SMARTer™ RACE cDNA Amplification kit (Clontech) following the manufacturer's protocol. Primer sequences are presented in Supplementary Table S3.

Plasmids production and transfection. DNA products from 3′ RACE were purified from the gel bands and cloned using the TOPO® TA Cloning Reaction (Invitrogen, Life technologies) and sequenced. Plasmids were digested with *Xho*I and *Hind*III (New England Biolabs® *Inc.*) to extract the Rac1-3′ UTR pA1 and pA2, which were inserted into pEGFP-C1 (Invitrogen). The resulting plasmid was submitted to site-direct mutagenesis [50] in order to eliminate the proximal PAS. The pA1 was mutated from ATTAAA to ACTAGA using in the PCR reaction the forward 5′ -CAGTCTAACTAGATTCAGCCCTAAAATACAAAGC-3′ and reverse 5′ -GCTGAATCTAGTTAGACTGTAAGTTGGAATTCTTA-3′ primers. Cortical neurons were transfected with the GFP constructs the day after plating (day 1), using jetPRIME (Polyplus) and following the manufacturer's protocol. The recombinant plasmid expressing full-length Rac1 plus the long 3′ UTR sequence, with pA1 mutated (pRP[Exp]-mCherry-EF1A > {Rac1 long form}) (mCherrie-rescue Rac1 long 3′ UTR) was ordered from Vectorbuilder.

Lentiviral production and transduction. The production of the shRNAs was based on the protocol [51] with adaptations. Lentiviral vector particles were produced using packaging HEK293T cells. Cells were transfected with three different plasmids: pSicoR was a gift from Tyler Jacks (Addgene plasmid # 11579) [52] carrying shRNA sequences and a green fluorescent protein (GFP) reporter tag, psPAX2 plasmid (Addgene plasmid # 12260, Didier Trono) carrying genes coding for lentiviral packaging proteins and pCMV-VSV-G was a gift from Bob Weinberg (Addgene plasmid # 8454) [53] containing genes coding for envelope proteins. The transfection reagent used was jetPRIME (Polyplus). Lentiviral particles were collected from the cell culture supernatants 2 days post-transfection and the viral titer was determined by Fluorescence-activated cell sorting (FACS). Cortical neurons were infected with the shRNA for the depletion of *Rac1* long 3′ UTR on the day after plating (day 1). A shRNA against dsRED fluorescent protein was used as infection control. The shRNA *Rac1* long 3′ UTR sequence (5′ -GGCGTTGAGTCCATATTTA-3′) was obtained by pSicoOligomaker 1.5 software (http://jacks-lab.mit.edu/protocol/psico). The shRNA sequence was cloned into the lentiviral pSicoR vector (Addgene) using *Hpa*I-*Xho*I cleavage sites.

Neuron transfection with calcium phosphate. Transfection of cultured cortical neurons with full length- Rac1-long 3′ UTR (pRP[Exp]-mCherry-EF1A > {Rac1 long form}) was performed in previously transduced neurons at 7 DIV using the calcium phosphate co-precipitation method as previously described, with minor modifications [48]. Briefly, 2 μg/coverslip of plasmid DNA were diluted in Tris-EDTA (TE) pH 7.3 and mixed with HEPES calcium chloride pH 7.2 (2.5 M $CaCl_2$, 10 mM HEPES). This DNA/TE/Calcium mix was added to a 2 × HEPES-buffered saline solution (270 mM NaCl, 10 mM KCl, 1.4 mM Na_2HPO_4, 11 mM Dextrose, 42 mM HEPES), pH 7.2. The precipitates were allowed to form for 30 min, with vortex mixing every 5 min, to ensure precipitates had similar small sizes. Meanwhile, coverslips with cultured neurons were incubated with cultured conditioned medium with 2 mM of kynurenic acid. The precipitate was added to each coverslip and incubated at 37 °C, 5% CO_2, for 3 h. Cells were then washed with acidic (10% CO_2) equilibrated culture medium containing 2 mM kynurenic acid and returned to the 37 °C/5% CO_2 incubator for 15 min. Finally, the medium was replaced with the initial culture-conditioned medium, and the cells were further incubated in a 37 °C/5%CO_2 incubator for 7 days.

Immunofluorescence (IF). Cells were fixed with 4% paraformaldehyde in MP buffer for the preservation of the cytoskeleton integrity. Afterwards, cells were permeabilized in 0.1% Triton X-100 in PBS for 10 min at room temperature and incubated in blocking solution for 1 h at room temperature, and probed with: for Figs. 4 and 5A- rat Ab anti-tubulin (ab6160, Abcam), overnight at 4 °C in blocking solution, and the secondary Alexa Fluor 647-conjugated goat anti-rat IgG (A21235, Molecular Probes) was incubated 60 min at RT in blocking solution; for Figure 5D - mouse Ab anti-GFP (11814460001, Roche, 1:500 dilution), and rabbit Ab anti-beta 3 Tubulin (ab18207, Abcam, final concentration 1 μg/mL) overnight at 4 °C, and the secondary Alexa Fluor 488-conjugated goat anti-mouse IgG (A11001, Molecular Probes, 1:500) and Alexa Fluor 647-conjugated donkey anti-rabbit IgG (A31573, Molecular Probes, 1:500) was incubated for 60 min at RT. The incubations were followed by serial washes with PBS (1x). 4′,6-Diamino-2-phenylindole hydrochloride (DAPI) (Molecular Probes)

was used to detect nuclei. The coverslips with the cells were mounted, and images were acquired in a Leica DMI 6000 B Microscope, using a x 20 objective with a 2048 × 2048 pixel resolution (Figs. 4e and 5A) or a laser scanning Confocal Microscope Leica (Wetzlar, Germany) SP2 AOBS SE, using an x 40 oil objective, NA 1.25, with a 1024 × 1024 pixel resolution, in a series of 0.23 um thick sections of entire neurons (Fig. 5D). Images were processed and analysed using FIJI package for Image J software [54].

Neuronal morphological analysis. Neurite outgrowth analysis was performed using the semi-automated tools of NeuronJ pluginto ImageJ software, following the developer's instructions. Brieflly, after the neurites were traced, the number and total length of neurites per cell were analysed. Results are representative of four independent experiments (Fig. 4) and three independent experiments (Fig. 5) [55,56].

Sholl analysis was performed as previously described using Bonfire scripts for MATLAB (Mathworks) [57]. After neurites were defined in

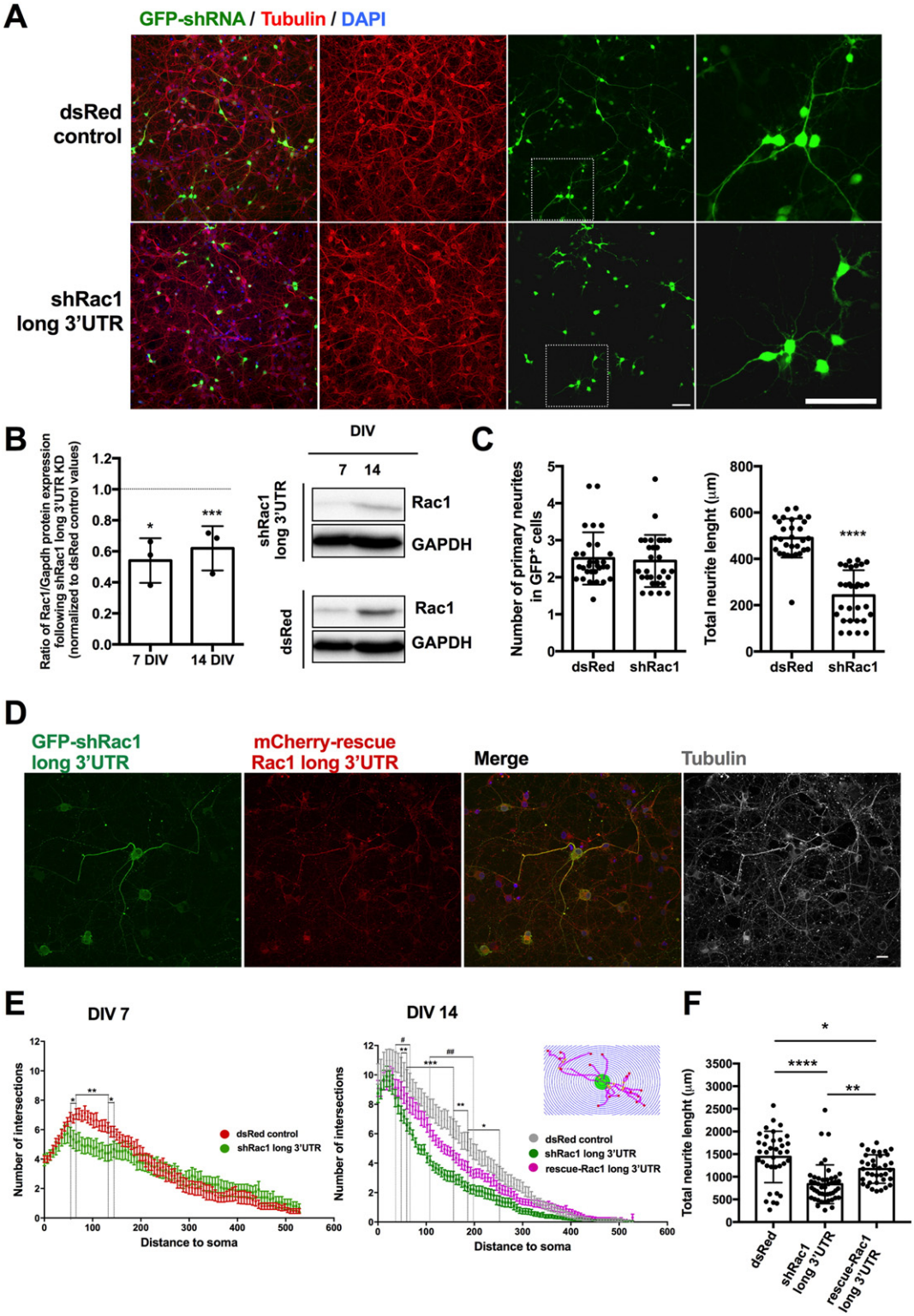

Neuron J, Bonfire was used to convert the data to SWC files, and the connectivity of tracings was defined in NeuronStudio, allowing the determination of each neuron dendritic arbour. Finally, Bonfire was used to perform the sholl analysis with a 6.0 μm ring interval, by drawing concentric circles around the cell body with incremental increased radii, and counting the number of times each circle crosses a neuritic segment. The number of intersections was represented as a function of the radial distance to the cell body.

Western-blot. Whole-cell lysates were prepared, resolved, and transferred with the iBlot gel transfer device (Life Technologies). Incubations with primary Ab diluted in PBST containing 5% non-fat dried milk were followed by washes with PBST, incubation with the appropriate secondary Abs in PBST/dried milk, and detection using enhanced luminescence (ECL Prime; Amersham/GE Healthcare). Abs used were mouse mAb anti-Rac1 (ab33186, Abcam), and anti-GAPDH (Mab6C5H yTest Ltd, 1:20000). Densitometric analysis with Image lab Software (Bio-Rad) has been performed to quantify signal intensity. Quantitative western blot results are represented as means of GAPDH levels (±SD) in treated cells, relative to normalized controls.

3.1. Statistically analysis

When only two groups were compared a Student's *t*-test was used (on a paired or unpaired fashion depending on the data). Comparisons between more than two groups were performed using one-way analysis of variance (ANOVA) followed by the Sidak multiple comparisons test. Sholl analysis curves were compared using a two-way ANOVA (transduction × number of intersections) corrected for multiple comparisons using the Sidak post-hoc test. Statistical significance was set at $P < 0.05$. The data are presented as mean ± standard deviation (±SD). All tests were conducted using the GraphPad-Prism software, version 7.00 for Mac Os X (GraphPad Software, Inc., San Diego, CA).

Supplementary data to this article can be found online at http://dx.doi.org/10.1016/j.bbagrm.2017.03.002.

Author contributions

AM, JBR and TS conceived and designed the project. SOB and AC designed, performed and interpreted the experiments. IP-C and JF performed and interpreted the *in silico* experiments. JB AL, JMR conducted most of the neuronal cell culture work. TS designed the neuronal experiments. JBR and AM supervised and discussed the project. AM, JBR, TS, SB and AC wrote the manuscript.

Conflict of interest

The authors declare that they have no conflict of interest.

Transparency document

The Transparency document associated with this article can be found, in online version.

Acknowledgments

This work was funded by Norte-01-0145-FEDER-000008 - Porto Neurosciences and Neurologic Disease Research Initiative at I3S, supported by Norte Portugal Regional Operational Programme (NORTE 2020), under the PORTUGAL 2020 Partnership Agreement, through the European Regional Development Fund (ERDF) and NORTE-07-0124-FEDER-000003-Cell Homeostasis Tissue Organization and Organism Biology co-funded by ON.2—O Novo Norte, under the QREN, through FEDER - Fundo Europeu de Desenvolvimento Regional FEDER and FCT. AC and AL were funded by ON2-201304-CTO-I. TS was supported by Investigador FCT (IF/00875/2012), POPH and Fundo Social Europeu. IP-C is funded by a FCT post-doc fellowship (SFRH/BPD/107901/2015).

References

[1] A. Derti, P. Garrett-Engele, K.D. Macisaac, R.C. Stevens, S. Sriram, R. Chen, C.A. Rohl, J.M. Johnson, T. Babak, A quantitative atlas of polyadenylation in five mammals, Genome Res. 22 (2012) 1173–1183.
[2] B. Tian, J. Hu, H. Zhang, C.S. Lutz, A large-scale analysis of mRNA polyadenylation of human and mouse genes, Nucleic Acids Res. 33 (2005) 201–212.
[3] S.W. Flavell, T.K. Kim, J.M. Gray, D.A. Harmin, M. Hemberg, E.J. Hong, E. Markenscoff-Papadimitriou, D.M. Bear, M.E. Greenberg, Genome-wide analysis of MEF2 transcriptional program reveals synaptic target genes and neuronal activity-dependent polyadenylation site selection, Neuron 60 (2008) 1022–1038.
[4] A. Curinha, S. Oliveira Braz, I. Pereira-Castro, A. Cruz, A. Moreira, Implications of polyadenylation in health and disease, Nucleus 5 (2014) 508–519.
[5] C.S. Lutz, A. Moreira, Alternative mRNA polyadenylation in eukaryotes: an effective regulator of gene expression, Wiley Interdiscip. Rev. RNA 2 (2011) 22–31.
[6] B. Tian, J.L. Manley, Alternative cleavage and polyadenylation: the long and short of it, Trends Biochem. Sci. 38 (2013) 312–320.
[7] D.C. Di Giammartino, K. Nishida, J.L. Manley, Mechanisms and consequences of alternative polyadenylation, Mol. Cell 43 (2011) 853–866.
[8] R. Elkon, A.P. Ugalde, R. Agami, Alternative cleavage and polyadenylation: extent, regulation and function, Nat. Rev. Genet. 14 (2013) 496–506.
[9] P.J. Shepard, E.A. Choi, J. Lu, L.A. Flanagan, K.J. Hertel, Y. Shi, Complex and dynamic landscape of RNA polyadenylation revealed by PAS-Seq, RNA 17 (2011) 761–772.
[10] R. Elkon, J. Drost, G. van Haaften, M. Jenal, M. Schrier, J.A. Oude Vrielink, R. Agami, E2F mediates enhanced alternative polyadenylation in proliferation, Genome Biol. 13 (2012) R59.
[11] M. Hoque, Z. Ji, D. Zheng, W. Luo, W. Li, B. You, J.Y. Park, G. Yehia, B. Tian, Analysis of alternative cleavage and polyadenylation by 3′ region extraction and deep sequencing, Nat. Methods 10 (2013) 133–139.
[12] S. Lianoglou, V. Garg, J.L. Yang, C.S. Leslie, C. Mayr, Ubiquitously transcribed genes use alternative polyadenylation to achieve tissue-specific expression, Genes Dev. 27 (2013) 2380–2396.
[13] Y. Shi, Alternative polyadenylation: new insights from global analyses, RNA 18 (2012) 2105–2117.
[14] C. Mayr, D.P. Bartel, Widespread shortening of 3′ UTRs by alternative cleavage and polyadenylation activates oncogenes in cancer cells, Cell 138 (2009) 673–684.
[15] R. Sandberg, J.R. Neilson, A. Sarma, P.A. Sharp, C.B. Burge, Proliferating cells express mRNAs with shortened 3′ untranslated regions and fewer microRNA target sites, Science 320 (2008) 1643–1647.

Fig. 5. *Rac1* longest 3′ UTR mRNA function in dendritic outgrowth of cortical neurons. A. Representative images of primary cortical neurons at DIV 7 infected with a lentivirus carrying a shRNA targeting the *Rac1* longest 3′ UTR mRNA isoform and containing a GFP tag (shRac1 longest 3′ UTR). Infection was controlled using an shRNA for dsRed. Efficiency of transduction: dsRED - 23%, shRac1 - 22%. Scale bars represent 100 μm. B. The effect of *Rac1* longest 3′ UTR mRNA knockdown in Rac1 protein production in primary cortical neurons was quantified by western blot at DIV 7 and DIV 14. Results represent mean ± standard deviation (SD) for three independent experiments. Comparisons were performed against dsRed control values by one-way analysis of variance (ANOVA) followed by Sidak *multiple comparison post-hoc* tests ($^{*}p < 0.05$, $^{***}p < 0.001$). C. Changes in neuronal morphology resulting from *Rac1* longest 3′ UTR mRNA knockdown were quantified at DIV 7 by measuring the number of primary neurites and total neurite length. Results represent mean ± SD for three independent experiments and at least 10 cells per experiment. Comparisons were performed using a paired Student's *t*-test ($^{****}p < 0.0001$). D. Representative images of DIV 14 cortical primary neurons infected at DIV 1 with an shRNA targeting the *Rac1* longest 3′ UTR mRNA isoform and containing a GFP tag (shRac1 long 3′ UTR). At DIV 7 these cultures were transfected with a pRP[Exp]-mCherry-EF1A>{Rac1 long form} (mCherry-rescue Rac1 long 3′ UTR) construct to rescue the phenotype induced by shRac1 long 3′ UTR. Efficiency of transduction: shRac1 – 26%, rescueRac1 – 13%. Scale bar represent 20 μm. E. Sholl analysis at DIV 7 and DIV 14 quantifying changes in neurite branching under shRac1 long 3′ UTR control and branching increase at DIV 14 under mCherry-rescue *Rac1* long 3′ UTR. A series of concentric rings calibrated at 6 μm intervals were superimposed on each neuronal cell body, the number of dendritic intersections within each concentric ring was counted, and the dendritic length was measured. Results represent mean ± standard deviation (SD) for three independent experiments. Data was analyzed by two-way analysis of variance (ANOVA) corrected for multiple comparisons using the Sidak *multiple comparison post-hoc* test, $^{***}p < 0.001$, $^{**}p < 0.01$ or $^{*}p < 0.05$ when comparing the shRac1 and rescue-Rac1 conditions, and $^{\#}p < 0.05$ or $^{\#\#}p < 0.01$ when comparing dsRed and rescue-Rac1 conditions. F. Total neurite length at DIV 14. Results represent mean ± standard deviation (SD) for three independent experiments with at least 10 neurons per condition. Comparisons were performed by one-way analysis of variance (ANOVA) followed by Sidak *multiple comparison post-hoc* tests $^{****}p < 0.0001$, $^{**}p < 0.01$, $^{*}p < 0.05$). Tubulin was used to label microtubules, 4′-6-diamidino-2-phenylindole (DAPI) for nucleus.

[16] Z. Ji, J.Y. Lee, Z. Pan, B. Jiang, B. Tian, Progressive lengthening of 3′ untranslated regions of mRNAs by alternative polyadenylation during mouse embryonic development, Proc. Natl. Acad. Sci. U. S. A. 106 (2009) 7028–7033.
[17] P. Smibert, P. Miura, J.O. Westholm, S. Shenker, G. May, M.O. Duff, D. Zhang, B.D. Eads, J. Carlson, J.B. Brown, R.C. Eisman, J. Andrews, T. Kaufman, P. Cherbas, S.E. Celniker, B.R. Graveley, E.C. Lai, Global patterns of tissue-specific alternative polyadenylation in Drosophila, Cell Rep. 1 (2012) 277–289.
[18] G. Singh, G. Pratt, G.W. Yeo, M.J. Moore, The clothes make the mRNA: past and present trends in mRNP fashion, Annu. Rev. Biochem. 84 (2015) 325–354.
[19] P.A. Pinto, T. Henriques, M.O. Freitas, T. Martins, R.G. Domingues, P.S. Wyrzykowska, P.A. Coelho, A.M. Carmo, C.E. Sunkel, N.J. Proudfoot, A. Moreira, RNA polymerase II kinetics in polo polyadenylation signal selection, EMBO J. 30 (2011) 2431–2444.
[20] B.D. Berkovits, C. Mayr, Alternative 3′ UTRs act as scaffolds to regulate membrane protein localization, Nature 522 (2015) 363–367.
[21] C. Mayr, Evolution and biological roles of alternative 3′ UTRs, Trends Cell Biol. 26 (2016) 227–237.
[22] H. Zhang, J.Y. Lee, B. Tian, Biased alternative polyadenylation in human tissues, Genome Biol. 6 (2005) R100.
[23] P. Miura, S. Shenker, C. Andreu-Agullo, J.O. Westholm, E.C. Lai, Widespread and extensive lengthening of 3′ UTRs in the mammalian brain, Genome Res. 23 (2013) 812–825.
[24] J.M. Taliaferro, M. Vidaki, R. Oliveira, S. Olson, L. Zhan, T. Saxena, E.T. Wang, B.R. Graveley, F.B. Gertler, M.S. Swanson, C.B. Burge, Distal alternative last exons localize mRNAs to neural projections, Mol. Cell 61 (2016) 821–833.
[25] K.C. Martin, A. Ephrussi, mRNA localization: gene expression in the spatial dimension, Cell 136 (2009) 719–730.
[26] J.J. An, K. Gharami, G.Y. Liao, N.H. Woo, A.G. Lau, F. Vanevski, E.R. Torre, K.R. Jones, Y. Feng, B. Lu, B. Xu, Distinct role of long 3′ UTR BDNF mRNA in spine morphology and synaptic plasticity in hippocampal neurons, Cell 134 (2008) 175–187.
[27] J. Dubnau, A.S. Chiang, L. Grady, J. Barditch, S. Gossweiler, J. McNeil, P. Smith, F. Buldoc, R. Scott, U. Certa, C. Broger, T. Tully, The staufen/pumilio pathway is involved in Drosophila long-term memory, Curr. Biol. 13 (2003) 286–296.
[28] J. Zhong, T. Zhang, L.M. Bloch, Dendritic mRNAs encode diversified functionalities in hippocampal pyramidal neurons, BMC Neurosci. 7 (2006) 17.
[29] K. Limback-Stokin, E. Korzus, R. Nagaoka-Yasuda, M. Mayford, Nuclear calcium/calmodulin regulates memory consolidation, J. Neurosci. 24 (2004) 10858–10867.
[30] M. Giustetto, A.N. Hegde, K. Si, A. Casadio, K. Inokuchi, W. Pei, E.R. Kandel, J.H. Schwartz, Axonal transport of eukaryotic translation elongation factor 1alpha mRNA couples transcription in the nucleus to long-term facilitation at the synapse, Proc. Natl. Acad. Sci. U. S. A. 100 (2003) 13680–13685.
[31] P. Madaule, R. Axel, A novel ras-related gene family, Cell 41 (1985) 31–40.
[32] X.R. Bustelo, V. Sauzeau, I.M. Berenjeno, GTP-binding proteins of the Rho/Rac family: regulation, effectors and functions in vivo, Bioessays 29 (2007) 356–370.
[33] P. Aspenstrom, A. Ruusala, D. Pacholsky, Taking Rho GTPases to the next level: the cellular functions of atypical Rho GTPases, Exp. Cell Res. 313 (2007) 3673–3679.
[34] D. Bar-Sagi, A. Hall, Ras and rho GTPases: a family reunion, Cell 103 (2000) 227–238.
[35] C.C. Smithers, M. Overduin, Structural mechanisms and drug discovery prospects of rho GTPases, Cell 5 (2016).
[36] E.E. Govek, S.E. Newey, L. Van Aelst, The role of the rho GTPases in neuronal development, Genes Dev. 19 (2005) 1–49.
[37] M.L. Feltri, U. Suter, J.B. Relvas, The function of rho GTPases in axon ensheathment and myelination, Glia 56 (2008) 1508–1517.
[38] T. Thurnherr, Y. Benninger, X. Wu, A. Chrostek, S.M. Krause, K.A. Nave, R.J. Franklin, C. Brakebusch, U. Suter, J.B. Relvas, Cdc42 and Rac1 signaling are both required for and act synergistically in the correct formation of myelin sheaths in the CNS, J. Neurosci. 26 (2006) 10110–10119.
[39] J. Zhao, L. Hyman, C. Moore, Formation of mRNA 3′ ends in eukaryotes: mechanism, regulation, and interrelationships with other steps in mRNA synthesis, Microbiol. Mol. Biol. Rev. 63 (1999) 405–445.
[40] N.J. Proudfoot, Ending the message: poly(A) signals then and now, Genes Dev. 25 (2011) 1770–1782.
[41] Z.X. Luo, C.X. Yuan, Q.J. Meng, Q. Ji, A Jurassic eutherian mammal and divergence of marsupials and placentals, Nature 476 (2011) 442–445.
[42] L. Velten, S. Anders, A. Pekowska, A.I. Jarvelin, W. Huber, V. Pelechano, L.M. Steinmetz, Single-cell polyadenylation site mapping reveals 3′ isoform choice variability, Mol. Syst. Biol. 11 (2015) 812.
[43] M.C. Raff, C. Ffrench-Constant, R.H. Miller, Glial cells in the rat optic nerve and some thoughts on remyelination in the mammalian CNS, J. Exp. Biol. 132 (1987) 35–41.
[44] K.C. Vadodaria, C. Brakebusch, U. Suter, S. Jessberger, Stage-specific functions of the small rho GTPases Cdc42 and Rac1 for adult hippocampal neurogenesis, J. Neurosci. 33 (2013) 1179–1189.
[45] M. Kearse, R. Moir, A. Wilson, S. Stones-Havas, M. Cheung, S. Sturrock, S. Buxton, A. Cooper, S. Markowitz, C. Duran, T. Thierer, B. Ashton, P. Meintjes, A. Drummond, Geneious Basic: an integrated and extendable desktop software platform for the organization and analysis of sequence data, Bioinformatics 28 (2012) 1647–1649.
[46] K.D. McCarthy, J. de Vellis, Preparation of separate astroglial and oligodendroglial cell cultures from rat cerebral tissue, J. Cell Biol. 85 (1980) 890–902.
[47] Y.A. Syed, A.S. Baer, G. Lubec, H. Hoeger, G. Widhalm, M.R. Kotter, Inhibition of oligodendrocyte precursor cell differentiation by myelin-associated proteins, Neurosurg. Focus. 24 (2008), E5. .
[48] A.C. Lobo, J.R. Gomes, T. Catarino, M. Mele, P. Fernandez, A.R. Inacio, B.A. Bahr, A.E. Santos, T. Wieloch, A.L. Carvalho, C.B. Duarte, Cleavage of the vesicular glutamate transporters under excitotoxic conditions, Neurobiol. Dis. 44 (2011) 292–303.
[49] B. Manadas, A.R. Santos, K. Szabadfi, J.R. Gomes, S.D. Garbis, M. Fountoulakis, C.B. Duarte, BDNF-induced changes in the expression of the translation machinery in hippocampal neurons: protein levels and dendritic mRNA, J. Proteome Res. 8 (2009) 4536–4552.
[50] L. Zheng, U. Baumann, J.L. Reymond, An efficient one-step site-directed and site-saturation mutagenesis protocol, Nucleic Acids Res. 32 (2004), e115. .
[51] G. Tiscornia, O. Singer, I.M. Verma, Production and purification of lentiviral vectors, Nat. Protoc. 1 (2006) 241–245.
[52] A. Ventura, A. Meissner, C.P. Dillon, M. McManus, P.A. Sharp, L. Van Parijs, R. Jaenisch, T. Jacks, Cre-lox-regulated conditional RNA interference from transgenes, Proc. Natl. Acad. Sci. U. S. A. 101 (2004) 10380–10385.
[53] S.A. Stewart, D.M. Dykxhoorn, D. Palliser, H. Mizuno, E.Y. Yu, D.S. An, D.M. Sabatini, I.S. Chen, W.C. Hahn, P.A. Sharp, R.A. Weinberg, C.D. Novina, Lentivirus-delivered stable gene silencing by RNAi in primary cells, RNA 9 (2003) 493–501.
[54] J. Schindelin, I. Arganda-Carreras, E. Frise, V. Kaynig, M. Longair, T. Pietzsch, S. Preibisch, C. Rueden, S. Saalfeld, B. Schmid, J.Y. Tinevez, D.J. White, V. Hartenstein, K. Eliceiri, P. Tomancak, A. Cardona, Fiji: an open-source platform for biological-image analysis, Nat. Methods 9 (2012) 676–682.
[55] J. Popko, A. Fernandes, D. Brites, L.M. Lanier, Automated analysis of neuronJ tracing data, Cytometry A 75 (2009) 371–376.
[56] J.R. Gomes, R.S. Nogueira, M. Vieira, S.D. Santos, J.P. Ferraz-Nogueira, J.B. Relvas, M.J. Saraiva, Transthyretin provides trophic support via megalin by promoting neurite outgrowth and neuroprotection in cerebral ischemia, Cell Death Differ. 23 (2016) 1749–1764.
[57] C.G. Langhammer, M.L. Previtera, E.S. Sweet, S.S. Sran, M. Chen, B.L. Firestein, Automated Sholl analysis of digitized neuronal morphology at multiple scales: whole cell Sholl analysis versus Sholl analysis of arbor subregions, Cytometry A 77 (2010) 1160–1168.